LINGLEY, D. J., SHAW, R. A., WOODS, M. & KRISHNAMURTHY, S. S. (1978). *Phosphorus Sulfur*, **4**, 379-382.
MANI, N. V., AHMED, F. R. & BARNES, W. H. (1965). *Acta Cryst.* **19**, 693-698.
MANI, N. V., AHMED, F. R. & BARNES, W. H. (1966). *Acta Cryst.* **21**, 375-382.
MARTIN, J. & ROBERT, J. B. (1981). *Org. Magn. Reson.* **15**, 87-93.
MOSTELLER, F., ROURKE, R. E. K. & THOMAS, J. B. JR (1970). *Probability with Statistical Applications*, p. 345. Reading, Massachusetts: Addison-Wesley.
NYGAARD, L., BOJESEN, I., PEDERSEN, T. & RASTRUP-ANDERSEN, J. (1968). *J. Mol. Struct.* **2**, 209-215.
PARKES, H. G. & SHAW, R. A. (1984). Unpublished results.
RAMACHANDRAN, K. & ALLEN, C. W. (1983). *Inorg. Chem.* **22**, 1445-1448.
SCHMUTZ, J. L. & ALLCOCK, H. R. (1975). *Inorg. Chem.* **14**, 2433-2438.
SHAW, R. A. (1976). *Z. Naturforsch. Teil B*, **31**, 641-667.
SHAW, R. A. (1977). *Proceedings of First International Congress on Phosphorus Compounds*, Rabat, pp. 35-50. Institut Mondial du Phosphate.
SHAW, R. A., FITZSIMMONS, B. W. & SMITH, D. C. (1962). *Chem. Rev.* **62**, 247-281.
SHAW, R. A. & NABI, S. N. (1981). *ACS Symp. Ser.* **171**, 307-310.
SHELDRICK, G. M. (1976). *SHELX*76. A program for automatic solution of crystal structures. Univ. of Cambridge.
SHELDRICK, G. M. (1984). *SHELX*84. Personal communication.
STEWART, R. F., DAVIDSON, E. R. & SIMPSON, W. T. (1965). *J. Chem. Phys.* **42**, 3175-3187.
WARRENT, R. W., CAUGHLAN, C. N., HARGIS, J. H., YEE, K. C. & BENTRUDE, W. G. (1978). *J. Org. Chem.* **43**, 4266-4270.
WHITE, D. W. (1971). *Phosphorus*, **1**, 33-39.
WIECZOREK, M. W. (1980). *Phosphorus Sulfur*, **9**, 137-148.

Acta Cryst. (1985). B**41**, 131-135

Temperature-Dependence Studies of α-Oxalic Acid Dihydrate

BY Y. WANG,* C. J. TSAI AND W. L. LIU

Department of Chemistry, National Taiwan University, Taipei, Taiwan

AND L. D. CALVERT

Chemistry Division, NRC, Ottawa, Canada

(*Received* 4 *April* 1984; *accepted* 9 *October* 1984)

Abstract

Single-crystal X-ray analyses were made on oxalic acid dihydrate at five different temperatures - 300, 225, 170, 130, 100 K. A few selected peak profiles at various 2θ angles were monitored; the net intensities of the reflections increase on lowering the temperature as expected and this increase is more prominent for high-2θ-angle reflections than for low ones. The cell parameters contract anisotropically on lowering the temperature in the range studied [at 300 K: a = 6·120(2), b = 3·6058 (8), c = 12·057 (3) Å, β = 106·29 (2)°]. The atomic thermal vibrational amplitudes decrease with decreasing temperature. The deformation density maps were investigated at 100 K: there are bonding electron densities at the midpoints of bonds C-C and C-O, as expected; the lone-pair densities around the O atoms are revealed; the hydrogen bond between the oxalic acid molecule and the water molecule is interestingly demonstrated.

Introduction

The crystal structure of oxalic acid dihydrate was first studied by Ahmed & Cruickshank (1953). The charge density study of oxalic acid dihydrate at room temperature was then carried out by Coppens, Sabine, Delaplane & Ibers (1969). Recently, there have been several density studies at low temperature, *e.g.* Stevens & Coppens (1980), Dam, Harkema & Feil (1983), as a result of a common project on the density study of oxalic acid dihydrate at 100 K sponsored by the Commission on Charge, Spin and Momentum Densities of the International Union of Crystallography. The detailed comparison of the project was given in the report of Coppens *et al.* (1984). The present work presents the temperature dependence of the parameters in addition to the deformation density study at 100 K.

Experimental

A 0·34 mm diameter spherical oxalic acid crystal was cooled in a 5 mm diameter jet of cold nitrogen (from boiling liquid nitrogen); temperature of the jet adjusted from 95 K to room temperature by a heating resistor in the delivery arm; temperature of the crystal calibrated using a thermocouple with the tip at the crystal position. Intensities of the same unique set of reflections were collected with graphite-monochromated Mo $K\alpha$ radiation up to $2\theta = 90°$, except for the room-temperature ones which were collected up to 60° but with the whole sphere (four equivalent sets, total 2855 reflections). At 100 K, the additional $1\frac{1}{2}$ sets

* To whom correspondence should be addressed.

0108-7681/85/020131-05$01.50

(total 5655 reflections) were also collected. Interset agreement indices ($\sum \Delta I/I$) are 0·021 and 0·009 for observed reflections [$I \geq 2\sigma(I)$] at 100 and 300 K respectively. Three reference reflections (0,0,10, 426, 234) monitored every 50 reflections; intensities scaled accordingly (maximum variation 1·5%). Intensities collected using profile analysis of the $\theta/2\theta$ scan (Grant & Gabe, 1978); 2θ scan range (0·8+ 0·7 tan θ+0·8)°. Intensities corrected for absorption ($\mu r = 0{\cdot}03$) and Lorentz-polarization factors and then averaged over the equivalent sets. Refinements performed minimizing $\sum w(F_o - F_c)^2$ with weights from counting statistics. Data analyses all performed on a PDP-8 computer with the *NRCC* package (Larson & Gabe, 1978). Deformation maps were obtained on Tek 4012 and 4662 connected to the PDP-8A using the Fourier program modified by Tsai & Wang (1983).

Results

The cell parameters were obtained on the basis of 24 reflections in the range 50–60° in 2θ. The results are presented in Table 1. The temperature dependence of the parameters is shown in Fig. 1. The derivatives of dimensions *b* and *c* are more or less the same, whereas that of *a* is five times less. This indicates that the contraction with decreasing temperature is not isotropic with respect to the three unit-cell vectors which is probably related to the intermolecular packing.

A few reflections with various 2θ angles were chosen to study their profiles at different temperatures (100, 170, 225 K) at an interval of 0·01° in 2θ. Two of these ($\bar{3}$,0,15 and $\bar{1}\bar{1}$,0,3) are shown in Fig. 2. The net intensities shown in parentheses in the figure as I_{total} (I_{net}) increase with decreasing temperature as expected and the increase is much more prominent for high-angle reflections than for low-angle ones. The shapes of the reflections do not change within such a small range of temperature.

The fractional coordinates of oxalic acid dihydrate obtained at four temperatures have been deposited

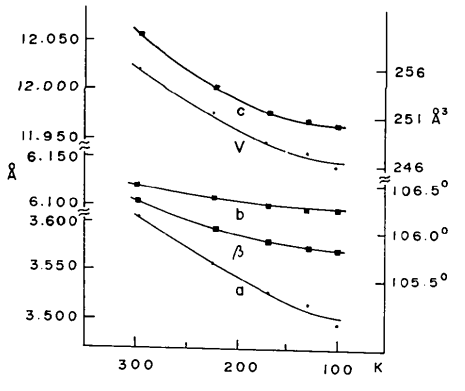

Fig. 1. Temperature dependence of the cell parameters.

Table 1. *Cell parameters at five temperatures for oxalic acid dihydrate*

T (K)	100	130	170	225	300
a (Å)	6·102 (2)	6·102 (2)	6·102 (2)	6·109 (1)	6·120 (2)
b (Å)	3·5011 (5)	3·5190 (4)	3·5298 (5)	3·5595 (4)	3·6058 (8)
c (Å)	11·964 (3)	11·973 (2)	11·978 (2)	12·008 (2)	12·057 (3)
β (°)	105·79 (2)	105·84 (2)	105·89 (2)	106·02 (2)	106·29 (2)
V (Å³)	245·95	247·33	248·13	250·97	255·39

together with additional results refined from high-order ($\sin\theta/\lambda \geq 0{\cdot}75$ Å^{-1}) reflections.* The coordinates do not change significantly except for the *y* coordinates of the heavy atoms. The interatomic distances at three temperatures (Fig. 3) showed no significant change for C–C, C–O(hydroxyl) and O–H distances; only the carbonyl C=O showed significant lengthening with decreasing temperature. This may be due to the uncorrected thermal motion (Wang, Blessing, Ross & Coppens, 1976) for room-temperature data; however, this is not true for other bond distances in the molecule and the thermal parameter of the carbonyl O is not different from those of the other atoms. One interesting feature can be noticed in the figure, which may correlate with the lengthening of carbonyl: the strong H bonding between the O atom of the water molecule [O(3)] and the hydroxyl H(1) is significantly shortened on lowering the temperature (1·513 *vs* 1·537 Å), as are the other H bonds formed by O(2), H(2) and O(3)

* Tables of fractional atomic coordinates and structure factors have been deposited with the British Library Lending Division as Supplementary Publication No. SUP 39788 (63 pp.). Copies may be obtained through The Executive Secretary, International Union of Crystallography, 5 Abbey Square, Chester CH1 2HU, England.

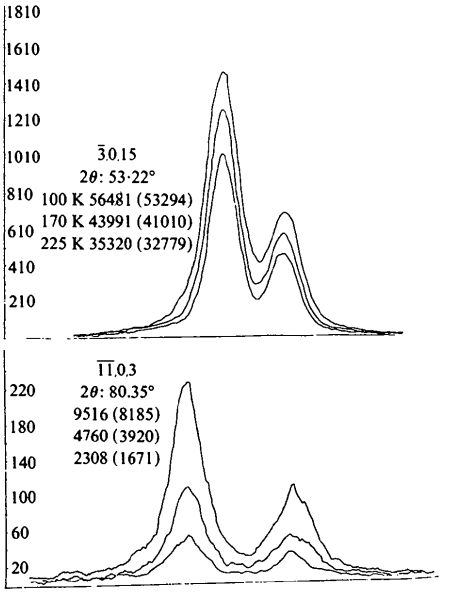

Fig. 2. Profiles of two selected reflections at 100, 170, 225 K; the total integrated counts and the net counts are given in the plot as I_{total} (I_{net}).

(1·985 *vs* 2·040 Å). This indicates that the H bonds are strengthened when the crystal is cooled.

The thermal parameters at five temperatures after least-squares refinements with full data and high-order data are listed in Table 2 with their agreement factors, scale factors and extinction coefficient g for full data (length in μm). The vibrational amplitudes along principal axes $\langle \bar{u}_i^2 \rangle$ have also been calculated and listed in Table 2. The Debye formula for cubic crystals was tried using the 170 K value to calculate the Debye temperature. $\bar{u}_i^2$ does decrease with decreasing temperature (Fig. 4); however, neither the linear approach nor the Debye formula could describe the trend. The comparison between the present thermal parameters and those of Stevens & Coppens (1980) gives ratios between our results and theirs of 1·121–1·154 in u_{11}, 1·211–1·296 in u_{22} and 1·133–1·183 in u_{33}. This disagreement among different sets of data was discussed in detail by Coppens *et al.* (1984). However, for this work, the range of high-order refinement ($\sin\theta/\lambda = 0{\cdot}75$–$1{\cdot}0$ Å^{-1}) is somewhat lower than theirs (1·0–1·2 Å^{-1}). As for the neutron diffraction data, the ratios for Koetzle & McMullan (1980) are slightly larger. The X–X maps presented here are the difference Fourier syntheses of independent atoms calculated from the high-order reflections ($\sin\theta/\lambda \geq 0{\cdot}75$ Å^{-1}) subtracted from all the reflections.

The deformation density for the molecular plane of oxalic acid is shown in Fig. 5. It does show some density at the midpoint of C–C, C–O and C=O. In addition, the lone-pair electron density can also be observed on two O atoms at the expected positions. The general features are quite comparable to those of earlier experimental ones (Stevens & Coppens, 1980; Dam, Harkema & Feil, 1983) and of theoretical calculations (Johansen, 1979). Figs. 6(*a*), 6(*b*) and 6(*c*) are the planes perpendicular to the molecular plane through the midpoints of bonds C–C, C=O and C–O. They all appear to have π-bonding character. The lone-pair electron density and the H bonds are particularly interesting when viewing the molecular plane of the water molecule (Fig. 7*a*) and the O(1)–H(1)···O(3) plane (7*b*) where the lone-pair

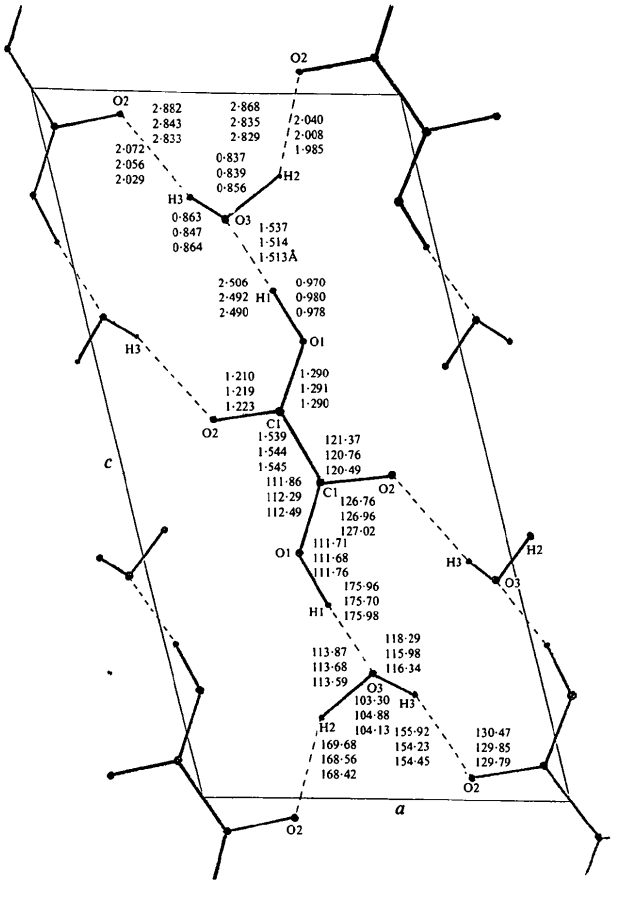

Fig. 3. Bond distances (Å) and angles (°) at 300 K (top), 170 K (middle) and 100 K (bottom).

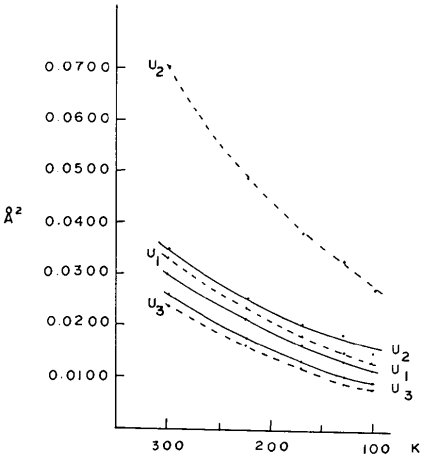

Fig. 4. Temperature dependence of the vibrational amplitudes. - - - O(1), —— C(1).

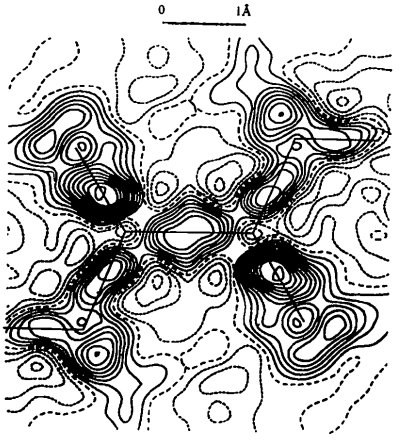

Fig. 5. Deformation map of the molecular plane of oxalic acid. [Here and in subsequent figures: contour interval 0·05 e Å^{-3}, zero and negative contours dashed, all data included ($\sin\theta/\lambda <$ 1·0 Å^{-1}).]

electrons of O(3) are apparently polarized towards the carboxyl H atom H(1). It is encouraging to see such a small effect with the X-ray diffraction method.

Discussion

The cell parameters of α-oxalic acid dihydrate do contract somewhat linearly in the range studied, but they do not shrink isotropically over the three unit-cell dimensions; in this case, *a* contracts the least while *b* and *c* contract about the same. The molecules are nearly perpendicular to the *b* axis; therefore, the cell is more contractable in this direction. The contraction of *c* may be accomplished by the shortening of the H bonds which is observed at lower temperature. The

Table 2. *Atomic thermal parameters* ($Å^2 \times 10^4$, *for* $H \times 10^3$) *and agreement indices*

$T = \exp[-2\pi^2(h^2a^{*2}U_{11}^2 + \cdots + 2hka^*b^*U_{12} + \cdots)]$.

		100 K	130 K	170 K	225 K	300 K
C(1)	U_{11}	118 (2)	144 (3)	168 (3)	214 (3)	304 (5)
	U_{22}	154 (3)	186 (4)	212 (4)	255 (4)	353 (7)
	U_{33}	97 (2)	117 (3)	136 (3)	178 (3)	266 (5)
	U_{12}	2 (2)	3 (3)	1 (3)	6 (3)	2 (5)
	U_{13}	33 (2)	36 (2)	40 (2)	53 (2)	85 (4)
	U_{23}	−3 (2)	−4 (3)	−4 (3)	−6 (3)	−9 (5)
O(1)	U_{11}	155 (2)	192 (3)	226 (3)	293 (3)	410 (4)
	U_{22}	247 (3)	305 (4)	343 (4)	430 (4)	621 (7)
	U_{33}	86 (2)	104 (2)	126 (2)	168 (2)	241 (4)
	U_{12}	56 (2)	73 (3)	86 (3)	111 (3)	153 (4)
	U_{13}	30 (1)	33 (2)	40 (2)	57 (2)	86 (3)
	U_{23}	11 (2)	12 (2)	14 (2)	15 (3)	19 (4)
O(2)	U_{11}	142 (2)	177 (3)	209 (3)	271 (3)	383 (4)
	U_{22}	232 (3)	281 (4)	325 (4)	411 (4)	601 (4)
	U_{33}	117 (2)	141 (2)	164 (2)	217 (2)	310 (4)
	U_{12}	56 (2)	73 (3)	87 (3)	115 (3)	167 (4)
	U_{13}	46 (1)	52 (2)	60 (2)	83 (2)	124 (3)
	U_{23}	7 (2)	9 (2)	13 (2)	17 (3)	20 (4)
O(3)	U_{11}	142 (2)	171 (3)	202 (3)	266 (3)	386 (5)
	U_{22}	252 (3)	317 (4)	348 (4)	443 (4)	643 (7)
	U_{33}	105 (2)	124 (2)	148 (2)	199 (2)	292 (4)
	U_{12}	40 (2)	52 (3)	56 (3)	78 (3)	115 (5)
	U_{13}	45 (1)	49 (2)	57 (2)	82 (2)	126 (4)
	U_{23}	13 (2)	18 (2)	20 (2)	29 (3)	46 (4)
H(1)	U	57 (3)	60 (4)	63 (4)	67 (4)	74 (4)
H(2)	U	49 (3)	50 (4)	55 (4)	61 (4)	81 (5)
H(3)	U	60 (4)	58 (4)	78 (5)	80 (4)	99 (6)
k_{obs}		0·06218 (1)	0·0618 (1)	0·0613 (1)	0·0614 (1)	0·0614 (2)
g		0·05 (1)	0·05 (2)	0·05 (2)	0·06 (2)	0·23 (3)
N_o		1680	1502	1439	1271	643
Nv		50	50	50	50	50
R		0·035	0·038	0·042	0·040	0·033
R_w		0·030	0·036	0·032	0·029	0·026
$\Delta I/I$		0·021				0·009
($\geq 2\sigma$)		(4522)				(2386)
N_m		6327				3301

Table 2 (*cont.*)

High-order refinement		100 K	130 K	170 K	225 K
C(1)	U_{11}	107 (1)	135 (2)	150 (3)	195 (3)
	U_{22}	145 (2)	180 (2)	197 (4)	243 (4)
	U_{33}	85 (1)	102 (2)	114 (2)	153 (3)
	U_{12}	19 (1)	25 (2)	28 (2)	36 (3)
	U_{13}	29 (2)	35 (1)	36 (2)	50 (2)
	U_{23}	2 (1)	0 (1)	3 (2)	2 (2)
O(1)	U_{11}	145 (1)	183 (2)	208 (3)	270 (3)
	U_{22}	231 (2)	293 (3)	327 (4)	418 (6)
	U_{33}	79 (1)	97 (2)	107 (2)	150 (3)
	U_{12}	53 (1)	72 (2)	81 (3)	114 (3)
	U_{13}	25 (2)	31 (1)	33 (2)	47 (2)
	U_{23}	9 (1)	12 (1)	15 (2)	19 (2)
O(2)	U_{11}	134 (1)	169 (2)	192 (3)	250 (3)
	U_{22}	215 (2)	279 (3)	311 (4)	402 (6)
	U_{33}	105 (1)	126 (2)	141 (2)	190 (3)
	U_{12}	64 (1)	83 (2)	97 (3)	127 (3)
	U_{13}	42 (1)	50 (1)	55 (2)	77 (2)
	U_{23}	8 (1)	12 (1)	17 (2)	19 (2)
O(3)	U_{11}	131 (1)	163 (2)	186 (3)	242 (3)
	U_{22}	224 (2)	281 (3)	314 (5)	298 (6)
	U_{33}	98 (1)	118 (2)	129 (2)	177 (3)
	U_{12}	31 (1)	41 (1)	50 (2)	63 (3)
	U_{13}	45 (1)	52 (1)	59 (1)	81 (2)
	U_{23}	13 (1)	17 (1)	21 (2)	25 (2)
k_{obs}		0·0653 (4)	0·0644 (5)	0·0669 (7)	0·0668 (8)
N_o		896	760	702	562
N_v		37	37	37	37
R		0·031	0·034	0·045	0·046
R_w		0·025	0·031	0·041	0·037

Vibrational amplitudes ($\times 10^5$) along the principal axes

		100 K	130 K	170 K	225 K	300 K
C(1)	U_1	1179	1310	1691	2139	3039
	U_2	1533	1905	2123	2569	3542
	U_3	945	998	1355	1770	2619
O(1)	U_1	1297	1511	1853	2344	3322
	U_2	2738	3369	3901	4942	7042
	U_3	851	953	1251	1670	2389
O(2)	U_1	1237	1354	1685	1919	2644
	U_2	2590	3214	3719	4759	6921
	U_3	1020	1168	1523	2218	3212
O(3)	U_1	1305	1464	1830	2372	3438
	U_2	2645	3102	3671	4729	6879
	U_3	972	1087	1425	1873	2712

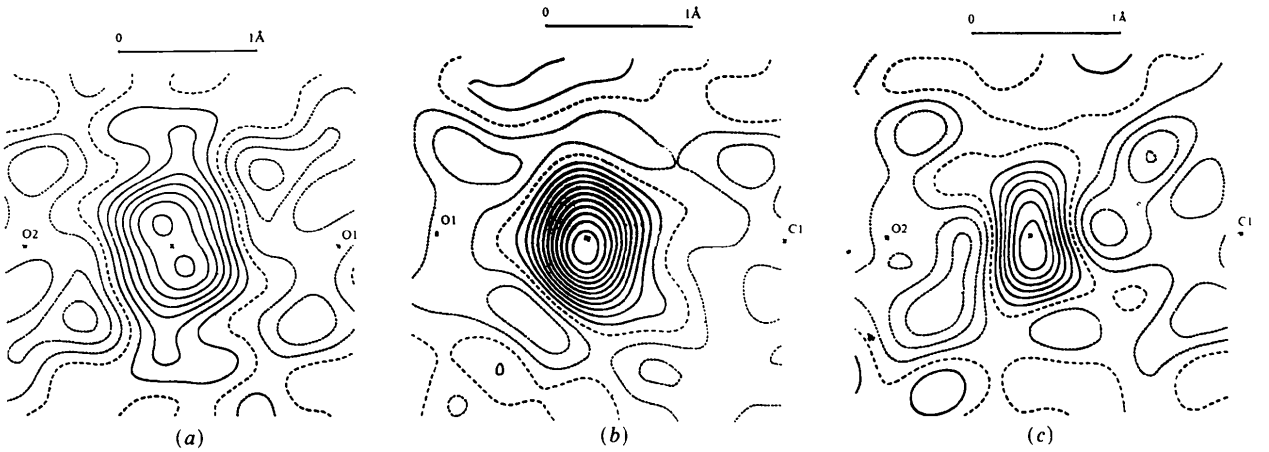

Fig. 6. Deformation map of the plane perpendicular to the molecular plane and bisecting bonds (*a*) C–C, (*b*) C=O(2), and (*c*) C—O(1).

interatomic distances and angles do not change significantly with temperature except for the C=O carbonyl bond which seems longer at lower temperature. The fractional coordinates at 100 K are comparable to those of earlier works (Dam, Harkema & Feil, 1983; Stevens & Coppens, 1980) within three standard deviations.

The vibrational amplitudes decrease with decreasing temperature as expected, but the discrepancies between the different sets of data (Coppens *et al.*, 1984) make it difficult to draw any conclusion. However, it was pointed out that these discrepancies may arise from the different temperatures of the samples at different laboratories or from the different treatment of the intensity data. This work presents the temperature-dependent studies on the same species with the same treatment at all the temperatures studied. Although the temperature may not be correct on the absolute scale, it at least shows the relative trends. As was mentioned by Coppens *et al.* (1984), it is fortunate that this does not affect the general features of the deformation density map; certainly it will affect some details in the map and peak heights. Qualitatively, the bonding features shown in Figs. 5-7 agree rather well with the corresponding figures of earlier work (Stevens & Coppens, 1980; Dam, Harkema & Feil, 1983). Nevertheless, there are still discrepancies in details, *e.g.* the π character shown in Fig. 6(*a*-*c*) is much more pronounced than that in Stevens & Coppens (1980). The maximum bond densities of C-O(1) (0·35) and O(1)-H(1) (0·29 e Å^{-3}) are the same as those in earlier work, but that of C-C (0·36) is much smaller and C-O(2) (0·58 e Å^{-3}) is larger than theirs. The lone-pair density of O(1) (0·37) and of O(2) (0·30, 0·25 e Å^{-3}) agrees better with those of Dam, Harkema & Feil (1983) than with those of Stevens & Coppens (1980).

The H bonding of O(1)-H(1)···O(3) is interestingly demonstrated in Fig. 7(*a*, *b*) with the lone pair on O(3) directly towards the carboxyl H atom which is quite comparable with the *ab initio* calculation (Johansen, 1979). The small charge deficiency in the deformation density map between the donor [O(3)] and the acceptor [H(1)] in the hydrogen bond mentioned by Stevens & Coppens (1980) is also observed; however, the positional parameters of the H atoms are from X-ray data which may not be sufficiently accurate for detailed discussion.

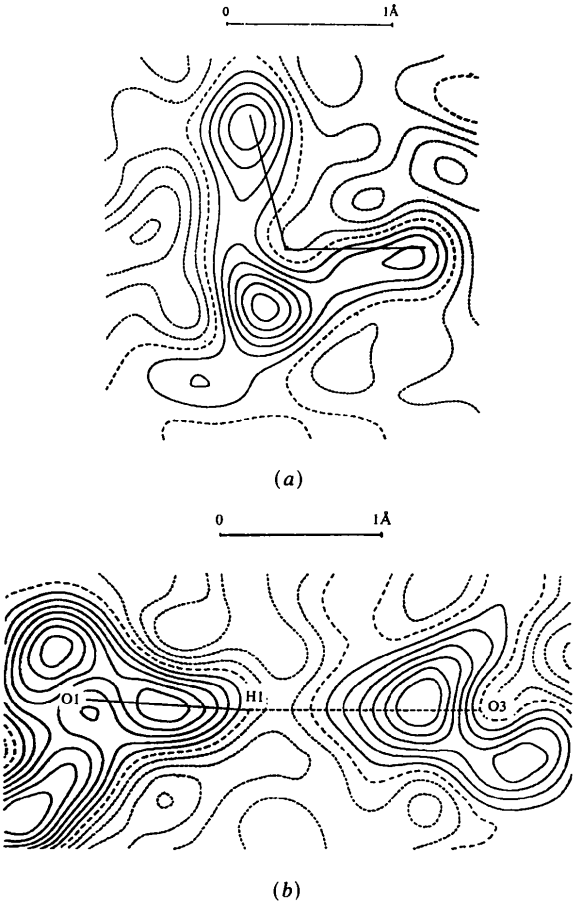

Fig. 7. Deformation maps of (*a*) the molecular plane of the water molecule and (*b*) the O(1)-H(1)···O(3) hydrogen-bonding plane.

References

AHMED, F. R. & CRUICKSHANK, D. W. J. (1953). *Acta Cryst.* **6**, 385-392.

COPPENS, P., DAM, J., HARKEMA, S., FEIL, D., FELD, R., LEHMANN, M. S., GODDARD, R., KRUGER, C., HELLNER, E., JOHANSEN, H., LARSEN, F. K., KOETZLE, T. F., MCMULLAN, R. K., MASLEN, E. N. & STEVENS, E. D. (1984). *Acta Cryst.* A**40**, 184-195.

COPPENS, P., SABINE, T. M., DELAPLANE, R. G. & IBERS, J. A. (1969). *Acta Cryst.* B**25**, 2451-2458.

DAM, J., HARKEMA, S. & FEIL, D. (1983). *Acta Cryst.* B**39**, 760-768.

GRANT, D. F. & GABE, E. J. (1978). *J. Appl. Cryst.* **11**, 114-120.

JOHANSEN, H. (1979). *Acta Cryst.* A**35**, 319-325.

KOETZLE, T. F. & MCMULLAN, R. K. (1980). Oxalic Acid Project Circular.

LARSON, A. C. & GABE, E. J. (1978). *Computing in Crystallography*, edited by H. SCHENK, R. OLTHOF-HAZEKAMP, H. VAN KONINGSVELD & G. C. BASSI, p. 81. Delft Univ. Press.

STEVENS, E. D. & COPPENS, P. (1980). *Acta Cryst.* B**36**, 1864-1876.

TSAI, J. & WANG, Y. (1983). International Summer School on Crystallographic Computing. Unpublished.

WANG, Y., BLESSING, R. H., ROSS, F. & COPPENS, P. (1976). *Acta Cryst.* B**32**, 572-578.